

Beating Reciprocity S/N Expectations in Narrow-bore Solids - The OptiMAS™ Probe, with Cryogenically Cooled Critical Circuit Components (C⁵)

Leyu Li, Siddarth Shevgoor, George Entzminger, J. B. Spitzmesser, Jennifer R. Doty, Vince Cothran, Chunjiang Xiao, Kranti Shevgoor, Jatin Kulkarni, Laura L. Holte, and F. David Doty

Doty Scientific, Columbia, SC

High-performance OptiMAS™ Circuit Innovations

INTRODUCTION AND BACKGROUND

The primary objectives of this development effort for advancing the state of the art of solids probes for H/X/Y MAS applications in narrow-bore (NB, also called standard bore, SB) magnets at the highest available fields are:

1. Increase S/N
2. Increase rf field strengths on the LF and MF channels
3. Include a high-performance Magic Angle Gradient (MAG) coil
4. Permit automatic sample change and fast MAS
5. Maintain compatibility with XC coils for ultra low rf sample heating
6. Allow ³H lock on a 4th channel
7. Permit full-range, multi-nuclear tuning
8. Enable extended VT operation to below 100 K

It has been nearly three decades since David Hoult so eloquently formulated the principle of reciprocity in NMR signal detection – essentially, the sensitivity in receiving an NMR signal is proportional to the “efficiency” of generating the rf B_1 by the receiver coil during the transmit pulse. Shortly thereafter, this principle was simplified into the following widely used and generally valid re-statements by several authors:

$$S/N \propto \frac{B_1 V_s}{\sqrt{P_T}} \propto \frac{V_s}{\sqrt{P_T}} \quad (1)$$

where P_T is the rf power needed to generate the rf field B_1 or the 90-degree pulse of length t_{90} within the sample volume V_s .

The above simplification of the principle of reciprocity understates the S/N advantage of cryo-probes because it assumes the noise power is simply proportional to the resistances (coil, capacitors, leads, sample, shields) within the circuit, whereas in fact noise is proportional to the product of resistance and its temperature. We report elsewhere our development efforts on CryoMAS H/X/Y probes for use in wide-bore magnets, where a factor of 4 to 9 increase in S/N appears possible, largely because the noise temperatures of the critical resistances in the circuit are greatly reduced. Unfortunately, cryogenic cooling of the sample coil in a VT MAS probe appears impractical in an NB magnet. However, cryogenic cooling of the critical LF/MF circuit components other than the sample coil appears practical, and this promises potential noise power reductions exceeding a factor of two, corresponding to a 40% increase in S/N.

RF Efficiency. We define rf circuit efficiency in a multi-resonance circuit as the fraction of rf power delivered from the probe port to the sample coil and sample, as in principle all other losses should be eliminated. RF circuit efficiencies in 3 to 5 mm triple-resonance “single-coil” MAS probes at very high fields are typically in the range of 25-35% at the LF) and 15-40% at the MF. While higher efficiencies on all channels have been achieved using a cross-coil for ¹H and a solenoid for the MF and LF, they are still generally in the range of 30-50% for both the LF and the MF. Such low efficiencies suggests there is considerable opportunity for noise reduction. Cooling the tuning elements external to the sample coil improves circuit efficiency (by improving their Qs), and we will show here that it should improve S/N even more than expected just on the basis of improved rf efficiency by reducing the noise temperature of these resistances.

S/N in Circuits at a Single Temperature. The S/N for a circuit in which all the losses are at a single temperature may be expressed as follows:

$$S/N = \left[\frac{h^2 \sqrt{2\pi} \mu_0}{12 k_B^{3/2}} \right] \frac{n_s \gamma I_s (I_s + 1) \sqrt{T_2}}{T_s \sqrt{T_R + T_p}} \left(\eta_{he} \eta_l Q_L V_s \right)^{1/2} \omega^{3/2} \quad (2)$$

where h is Planck’s constant, μ_0 is the permeability of free space, k_B is Boltzmann’s constant, n_s is the number of spins at resonance per unit volume, γ is the magnetogyric ratio, I_s is the spin quantum number, T_2 is the effective spin-spin relaxation time, T_s is the sample temperature, T_R is the temperature of the losses, T_p is the effective pre-amp noise temperature, η_{he} is the RF efficiency, η_l is the magnetic filling factor, Q_L is the loaded, matched circuit quality factor, V_s is the sample volume, and ω is the Larmor precession frequency, $\omega = \gamma B_0$.

A major problem with Eq. (2) is that in complex circuits, there may be many losses at various temperatures. Also, in complex circuits, it is not always easy to determine rf efficiency and magnetic filling factor unambiguously.

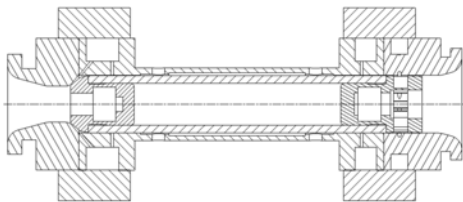


Figure 1. A novel drop-in spinner has been developed that is compatible with the Doty (XC) Cross-Coils, fast HR-MAS, and automatic sample change.

S/N in Complex Circuits with Losses at Various Temperatures

If we assume T_p is negligible compared to T_s (a reasonable assumption with tuned cryogenic preamps) and losses are confined to a single resistor R_n of temperature T_n in series with a lossless sample coil and capacitor, then for given NMR test conditions (sample, B_0 , T_s , T_n , and method), the following may be shown to follow from eq. (2):

$$S/N \propto \frac{B_1 V_s}{i \sqrt{R_n T_n}} \quad (3)$$

where i is the sample coil current. Since the Johnson noise voltage is proportional to $(R_n T_n)^{1/2}$, the signal voltage is proportional to $B_1 V_s / i$, and this statement of the principle of reciprocity is valid irrespective of the noise source temperature. Equation (3) is easily cast into the following form, which is more useful in practical probe design and evaluation, where power is dissipated in numerous losses of uniform temperature T_n :

$$S/N \propto \frac{B_1 V_s}{\sqrt{P_T T_n}} \quad (4)$$

where P_T is the total transmitter power required at the probe circuit port to generate B_1 . Both eqs. (3) and (4), without the T_n in the denominator, have been referred to as statements of the principle of reciprocity, as noted earlier. But clearly one cannot ignore the T_n factor when the various losses are at different temperatures.

Equation (4) is easily extended to handle the complex circuit where various losses are at different temperatures as follows:

$$S/N \propto \frac{B_1 V_s}{\sqrt{\sum P_n T_n}} \quad (5)$$

where P_n is the transmit power dissipated in the nth resistance of temperature T_n when generating B_1 , and the sum is over all resistances (in coils, capacitors, and leads) in the circuit. The easiest way to show this is to transform each loss into an equivalent resistor R_n in series with the sample coil. Then the noise voltage contribution from each resistor is proportional to $(R_n T_n)^{1/2}$, and its contribution to noise power (assuming $Q \gg 1$) is proportional to $R_n T_n / R_p$, where R_p is the equivalent parallel resistance of the coil circuit, which is a constant in the summation. The contribution of R_n to transmitter power, on the other hand, is simply proportional to R_n .

To use eq. (5), we first need to relate B_1 to the results from linear circuit simulation software, which can readily calculate the voltage v_i across the sample coil in complex circuits for a given input power. From basic relationships, the rf field generated by a coil of volume V_c can be shown to be given by the following:

$$B_1 = \frac{k_c v_i}{\omega \sqrt{L V_c}} \quad (6)$$

where k_c is a constant depending on the coil geometry. Substituting into eq. (5) gives:

$$S/N \propto \frac{v_i V_s}{\sqrt{L_c V_c \sum P_n T_n}} \quad (7)$$

where it is important to note that L_c is the inductance of the sample coil alone, not including leads.

Finally, since the standard circuit simulation tools do not include provisions for assigning noise temperatures to the various elements, it is necessary to adjust the various resistances appropriately. In high-Q tuned circuits, the component reactances are large compared to their series resistances; so the relative currents through the major components are independent of their resistances to first order, and the relative power dissipated in a circuit element is approximately proportional to its series resistance. Thus, a suitable way to correct the resistances for proper S/N calculation relative to S/N with the same resistances at 300 K is: (a) multiply all the resistances (in the coils, capacitors, leads, sample, and shields) by T_p / T_n , where T_n is a normalization temperature such that the total circuit Q is unchanged, and (b) multiply S/N by $\sqrt{500/T_n}$. Of course, the resistances of most elements at low temperatures are much less than at 300 K, and they must be determined by suitable methods. And when determined, the above method allows proper incorporation of T_n for accurate calculation of relative S/N using standard circuit simulation software.

Hence, when the same T_p , L_c , V_c , and coil type are used, the relative S/N of different complex circuits, with losses at various temperatures, is simply proportional to the voltage developed across the sample coil in the model for a given input power – assuming all the resistances have been properly scaled in proportion to their temperature.



Figure 2. A single torion turbine with an integral shroud is used in the drop-in spinner design.

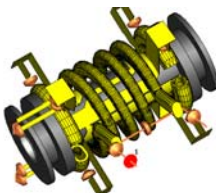


Figure 3. The ¹H XC and the LF/MF solenoid are shown here as simulated in CST MWS 5.0. The capacitors (8 for tuning, plus feed and balance) are represented by chamfered disks.

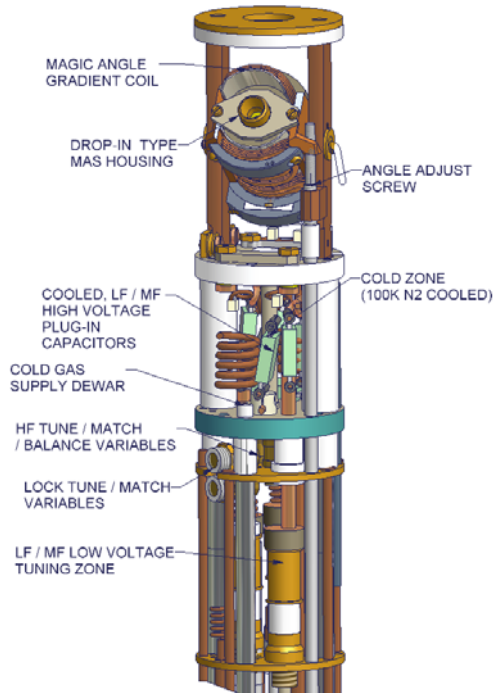


Figure 4: 3D view of prototype OptiMAS™ probe in progress, in which the critical circuit components are located in a Cold Zone just below the Spinner Zone. Cold nitrogen gas is introduced into this region via a small dewar. Most of this cooling gas exhausts upward, providing some cooling of the flexible leads to the sample coils but having little effect on the sample temperature, which is primarily established by the bearing gas temperature.

The spinner assembly may be flipped upward for automatic sample change when a novel, drop-in spinner design is used. (The novel turbine drive cap is shown below in Figure 2.)

The body tube (not shown) surrounding the probe is a thin-walled metallic dewar, which provides the insulation needed both for the cold zone and extended VT operation.

The variable capacitors are located in RT regions below the cold zone. The unique LF/MF circuit results in the losses associated with the relatively long leads to the variables being only a few percent of sample coil losses, and rf voltages in the tuning zone are low compared to the sample coil voltage to permit maximum LF and MF rf field strengths.

Building on the Proven XC Advantages

As in most of our solids H/X/Y circuits above 400 MHz, the OptiMAS probe uses a highly optimized cross-coil (XC) for ¹H and an outer solenoid for the LF and MF channels (see Figure 3) because of the strong advantages this approach offers in reducing decoupler heating by an order of magnitude, permitting higher decoupling in high-field MAS, and achieving higher S/N. For example, we have demonstrated S/N greater than 220 on glycine ¹³C for H/C/N tuning at 750 MHz – about twice the S/N of alternative solids probes for narrow bore magnets when in the triple configuration.

Alternative, fixed-tuned, circuits have permitted higher rf field strengths on the LF and MF channels (at least with smaller sample sizes) than our prior NB XC H/X/Y multi-nuclear circuits. The novel MF/LF OptiMAS circuit shown below in Figure 5 is expected to address the high-power requirement in solids in a more optimal manner without sacrificing multi-nuclear tuning.

As also shown in the perspective view of Figure 4, the critical MF/LF high-power tuning elements, indicated in Fig. 5 within the broken-line box, are immediately below the flexible (TRL1) connected to the sample solenoid. The impedance transformations in these high-power elements insure the currents, voltages, and SWR in TRL2, which connects these elements to the variables in the tuning zone, are relatively low, so losses in TRL2 are negligible. The new circuit also uses only large (3 mm x 11 mm x 15 mm), 2.5 kV, high-power capacitors in all the high-current paths, which imparts some additional Q stability, as needed in indirect experiments.

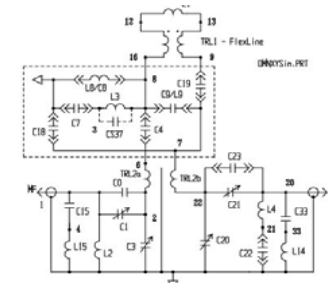


Figure 5: Double-tuned LF/MF Solenoid Circuit. The high-power tuning elements, indicated within the broken-line box, are located in the cold zone immediately below the spinner housing region. Losses below the cold zone are negligible.

Preliminary Results

A preliminary version of the OptiMAS probe, lacking several features (sample eject and MAG coil) is being built and will soon be tested to verify the S/N and rf power handling advantages of the novel MF/LF circuitry. Figure 6 illustrates the ¹H rf field for the 4 mm XC, as simulated using CST MWS 5.0 at 750 MHz, and Figure 7 shows the calculated close matching of field strength between the inner XC and the outer LF/MF solenoid. Experiments at 300 MHz are expected within a few weeks, followed by experiments at 500 MHz and then 750 MHz.

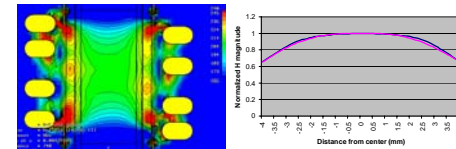


Figure 6. Plot with 2.5% contours of the B_1 magnitude in the YZ plane for the XC with a saline sample at 750 MHz. The outer solenoid is not driven at the high frequency.

CONCLUSIONS

Preliminary design, analyses, and simulations of a prototype solids probe design compatible with cryogenic cooling of the critical rf circuit components other than the sample coils have been successfully completed, and two related patent applications have been filed. Initial NMR tests are expected within a few weeks. Further work will focus primarily on perfecting automatic sample change, incorporating the MAG coil, and improving spectral resolution.

REFERENCES

1. F. D. Doty, “Probe Design and Construction.” *The Encycl. of NMR Vol. 6*, Wiley, 3753-3762, 1996.
2. F. D. Doty, G. Entzminger, and A. Yang, “Magnetism in HR NMR Probe Design, Part II: HR-MAS,” *Concepts in Magn. Reson.*, (4), 239-260, 1998.
3. F. D. Doty et al., “Reducing Decoupler Heating by an order of magnitude at 750 MHz,” presented at the Rocky Mountain Analytical Chem. Conf., Denver, 2004.

Acknowledgements: This work partially supported by NIH R43 EB00152-02.